Irreversible Inactivation of SARS-CoV-2 by Lectin Engagement with Two Glycan Clusters on the Spike Protein

Aakansha Nangarlia[1,2,#], Farah Fazloon Hassen[1], Gabriela Canziani[1], Praneeta Bandi[1], Choya Talukder[1], Fengwen Zhang[3,4], Douglas Krauth[5], Ebony N. Gary[6], David B. Weiner[6], Paul Bieniasz[3,4], Sonia Navas-Martin[5,7], Barry O'Keefe[8,9], Charles G. Ang[1*], Irwin Chaiken[1*]

[1]Department of Biochemistry and Molecular Biology, Drexel University College of Medicine, Philadelphia, Pennsylvania 19102, United States

[2]School of Biomedical Engineering, Science and Health Systems, Drexel University, Philadelphia, Pennsylvania 19102, United States

[3]Laboratory of Retrovirology, The Rockefeller University, New York, 10065, United States

[4]Howard Hughes Medical Institute, The Rockefeller University, New York, 10065, United States

[5]Department of Microbiology and Immunology, Drexel University College of Medicine, Philadelphia, Pennsylvania 19102, United States

[6]The Vaccine and Immunotherapy Center, Wistar Institute, Philadelphia, Pennsylvania, 19104, United States

[7]Center for Molecular Virology & Translational Neuroscience, Institute for Molecular Medicine & Infectious Disease

[8]Molecular Targets Program, Center for Cancer Research, National Cancer Institute, NIH, Frederick, Maryland, 21702, United States

[9]Natural Products Branch, Developmental Therapeutics Program, Division of Cancer Treatment and Diagnosis, National Cancer Institute, Frederick, Maryland, 21702, United States

[#]Current Affiliation: IQVIA Life Science Consulting.

*Please address correspondence to Charles G. Ang (cga26@drexel.edu) or Irwin Chaiken (imc23@drexel.edu)

KEYWORDS: Lectins, cyanovirin-N, griffithsin, microvirin, SARS-CoV-2, Spike, irreversible inactivation, virus inhibition, conformation, glycosylation, pseudovirus mutagenesis, glycan mapping, surface plasmon resonance, shedding.

Supporting Information

Index

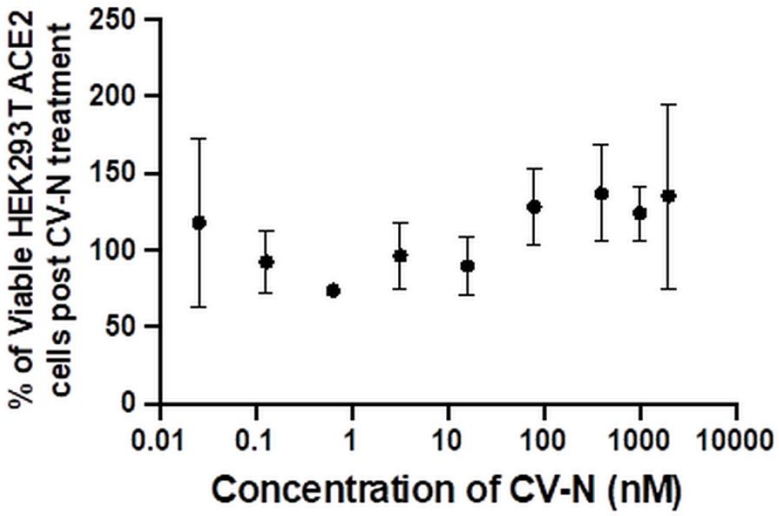

Figure S1: No cytotoxicity effects towards HEK293T ACE2 cells observed with CV-N. *The results from WST-1 assay shows 100% viability in HEK 293T cells post overnight CV-N treatment at concentrations up to 2000 nM. Data represent the mean of 3 independent experiments, and the error bars depict the standard deviation around the mean.*

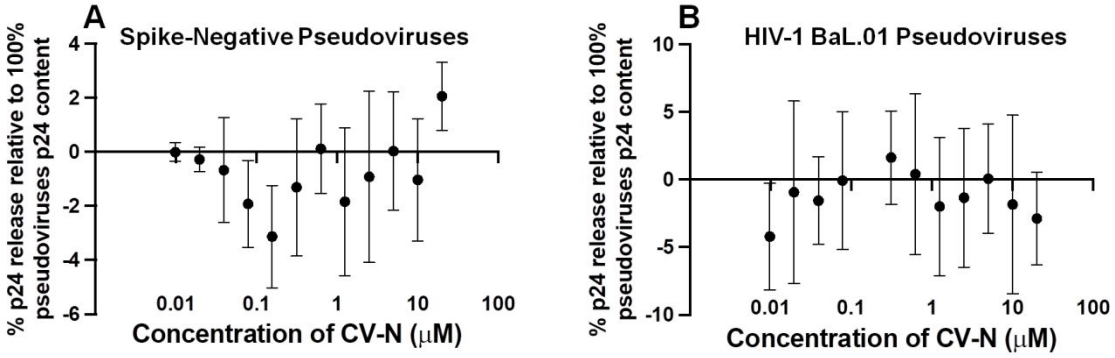

Figure S2: The lectin, CV-N, does not cause membrane disruption of Spike-Negative and HIV-1 BaL 01 pseudoviruses. *As compared to the p24 release observed with SARS-CoV-2 (**Fig S4**), CV-N did not cause release from non-Spike expressing (Spike-Negative, A), and HIV-1 BaL 01 (B) pseudoviruses. The control pseudoviruses contained similar p24 contents as the SARS-CoV-2 pseudoviruses used in this study.*

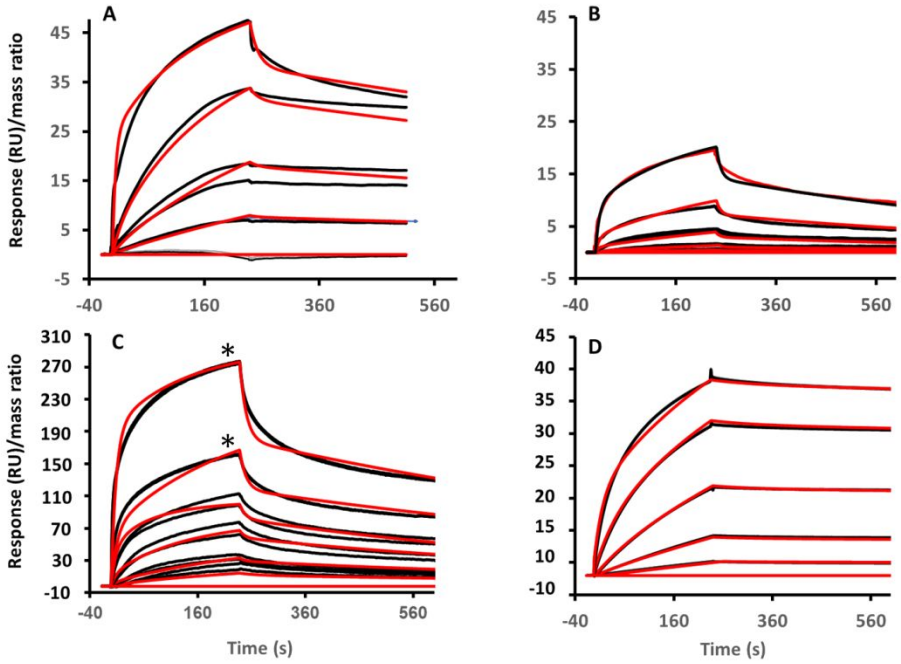

Figure S3: SPR-derived normalized dose response and analysis of S1 domain interactions with CV-N (A), CV-N [P51G] (B), GRFT (C) and soluble ACE2 (D). *S1-CV-N (A) and S1-CV-N [P51G] (B) interactions were best described by a two binding equilibrium/bivalent binding model. The S1-CV-N data fit was based on a dimer of dimers model without modification of the initial rate of CV-N binding (7.4-600 nM). On the other hand, S1-GRFT binding profiles (C) were fit to a bivalent binding model based on prior findings that bivalent GRFT dimer complexes can form, and we speculated that monovalent complexes may occur at high concentration (indicated by * where Rmax is 2-3 fold higher). S1-ACE2 binding (D) was described by a conformational change model (24.6-2000 nM). Black curves are experimental data and red curves are the corresponding fits.*

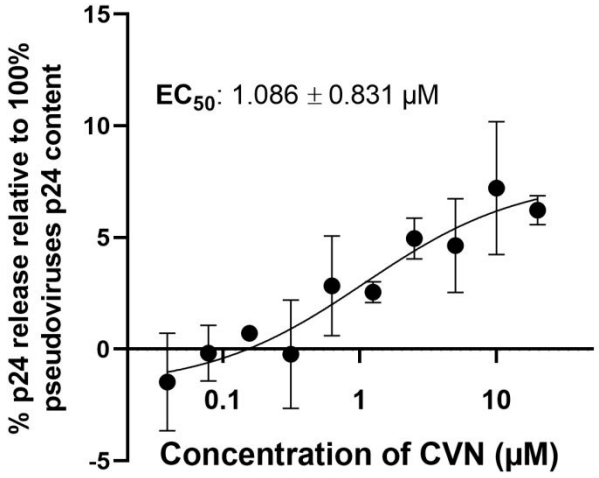

Figure S4: Membrane disruption of SARS-CoV-2 pseudovirus upon CV-N treatment. *Evaluation of p24 release from within pseudoviruses post CV-N treatment via a p24 ELISA assay shows that CV-N can cause membrane disruption of SARS-CoV-2 pseudoviruses in a dose-dependent manner. Data represent the mean of 3 independent experiments, and the error bars depict the standard deviation around the mean.*

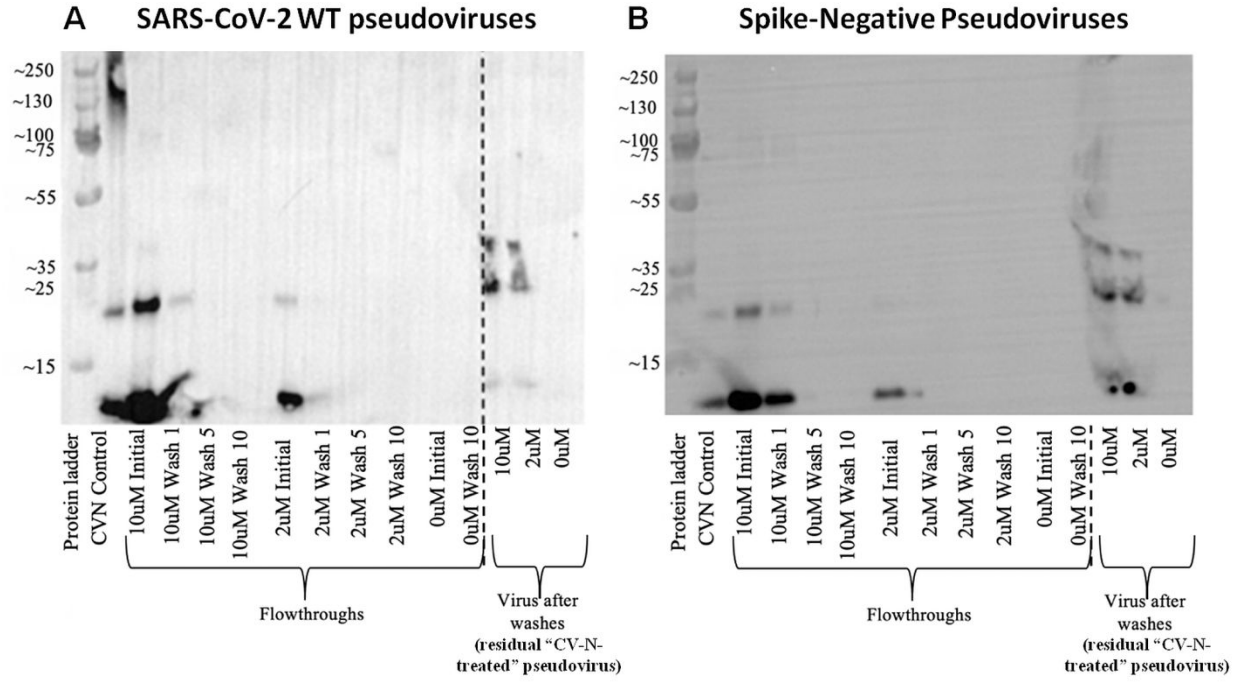

Figure S5: CV-N detection on residual "CV-N" treated SARS-CoV-2 and Spike-Negative pseudoviruses. *Western Blot (WB) analysis show that CV-N is detected on residual "CV-N-treated" pseudoviruses despite complete CV-N washout in the flow through for SARS-CoV-2 WT (A) and non envelope expressing (Spike-Negative) pseudoviruses (B).*

	CV-N in 20μL **WT Sample**	CV-N molecules per **WT Virion**
Residual CV-N after 0 Washes	40.9 ± 0.8 pg	**8.9 ± 0.2 molecules**
Residual CV-N after 1 Wash	41.6 ± 0.2 pg	**9.07 ± 0.05 molecules**
Residual CV-N after 5 Washes	5.44 ± 0.04 pg	**1.19 ± 0.01 molecules**
Residual CV-N after 10 Washes	2.488 ± 0.006 pg	**0.543 ± 0.001 molecules**

	CV-N in 20μL **N61D Sample**	CV-N molecules per **N61D Virion**
Residual CV-N after 0 Washes	46.4 ± 0.8 pg	**10.1 ± 0.2 molecules**
Residual CV-N after 1 Wash	41.2 ± 0.4 pg	**8.98 ± 0.08 molecules**
Residual CV-N after 5 Washes	2.63 ± 0.02 pg	**0.573 ± 0.004 molecules**
Residual CV-N after 10 Washes	<1.25 pg (0.41 ± 0.01 pg)	**<0.3 molecules (0.0906 ± 0.0001 molecules)**

Table S1: Quantification of residual CV-N after WT and N61D pseudovirus treatment and washout. *Detection of CV-N in WT and N61D pseudovirus samples after 2 hour CV-N treatment and washout was carried out by direct binding ELISA and comparison to a CV-N standard curve from 80-1.25 pg. For comparison, quantification of S1 protein for WT and N61D pseudovirus was also performed. WT: 3.05-3.25 ng S1; 95-102 molecules of S1 per virion or 31-34 trimers per virion. N61D: 2.06-2.42 ng S1; 64-76 molecules of S1 per virion or 21-25 trimers per virion. Per-virion calculations were based on testing 20μL samples containing 1ng/μL p24 worth of pseudovirus treated at 2μM CV-N, and a count of 2000 molecules of p24 per virion. Data shown are means and standard deviations from three independent experiments*

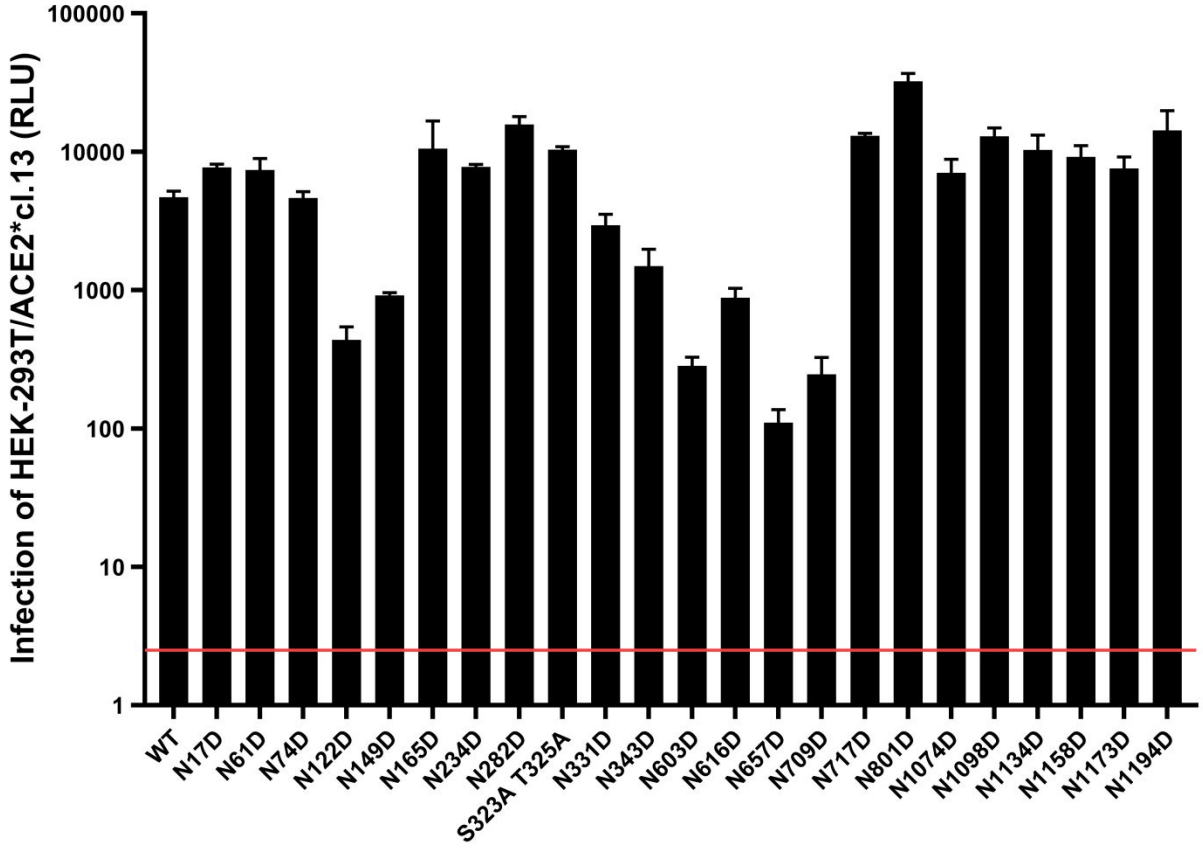

***Figure S6**: **Infectivity (Virus titration): Single-site SARS-CoV-2 glycan mutants.** To determine the effect of glycan-attachment site mutations on viral infectivity, we conducted a luciferase-based viral infectivity assay on a uniform 50 ng of p24 worth of pseudovirus. All mutants exhibited infectivity levels distinguishable from background/uninfected cells (indicated by red line), though individual infectivity levels varied. Data represent the mean of 3 independent experiments, and the error bars depict the standard deviation around the mean.*

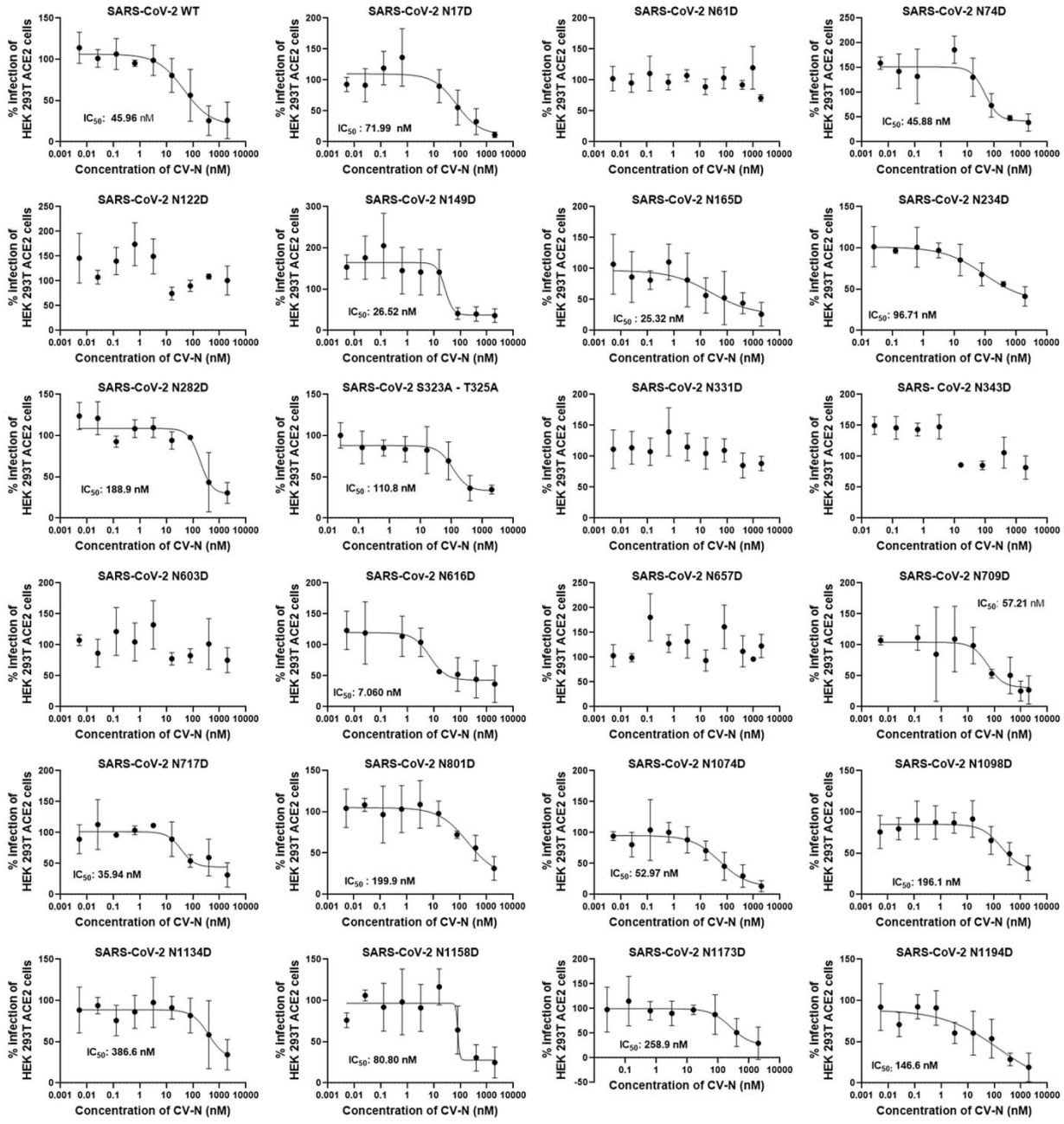

Figure S7: Dose-response infection inhibition of single-site glycan attachment site mutants by CV-N.

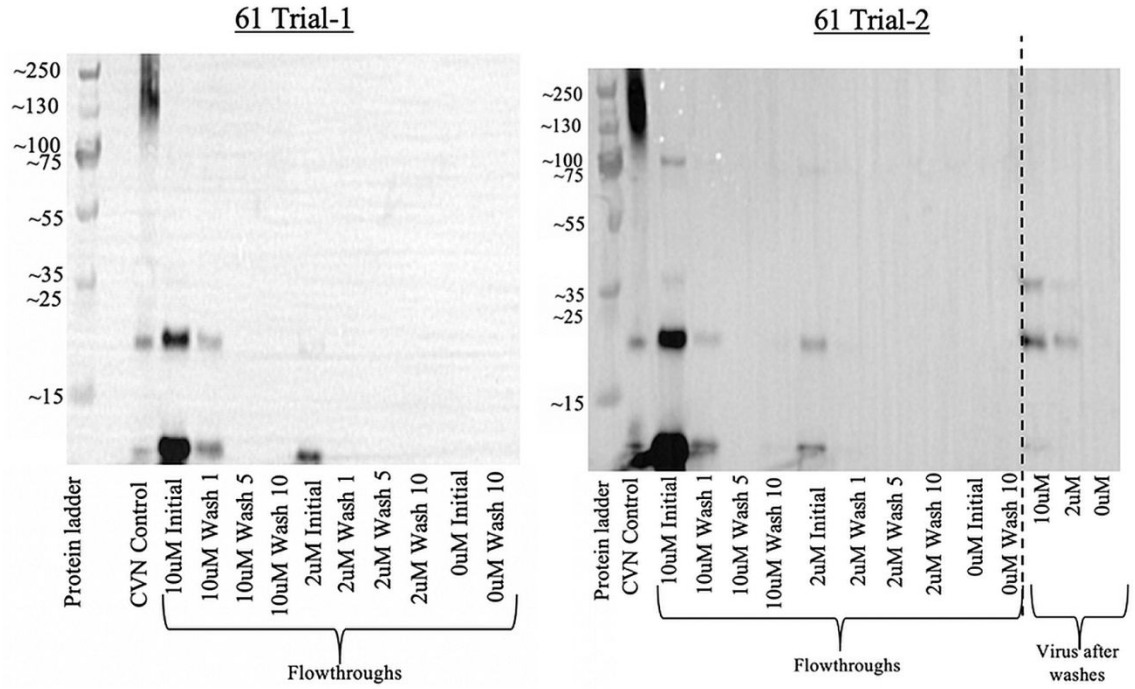

Figure S8: N61D - Western Blot for CV-N detection for Washout Experiments. *To confirm the washout of CV-N from the samples, Western Blot analysis was conducted to detect CV-N in the flow-through and post-treatment pseudoviruses sample. As shown in the images, all CV-N was washed out from the sample and remained undetectable in the flow through after wash 5, indicating a maximum washout of the CV-N by wash 10. Similar to WT and Spike Negative pseudoviruses after CV-N treatment (**Figure S5**), residual CV-N was detected on post-treatment mutant pseudoviruses even after ten washes.*

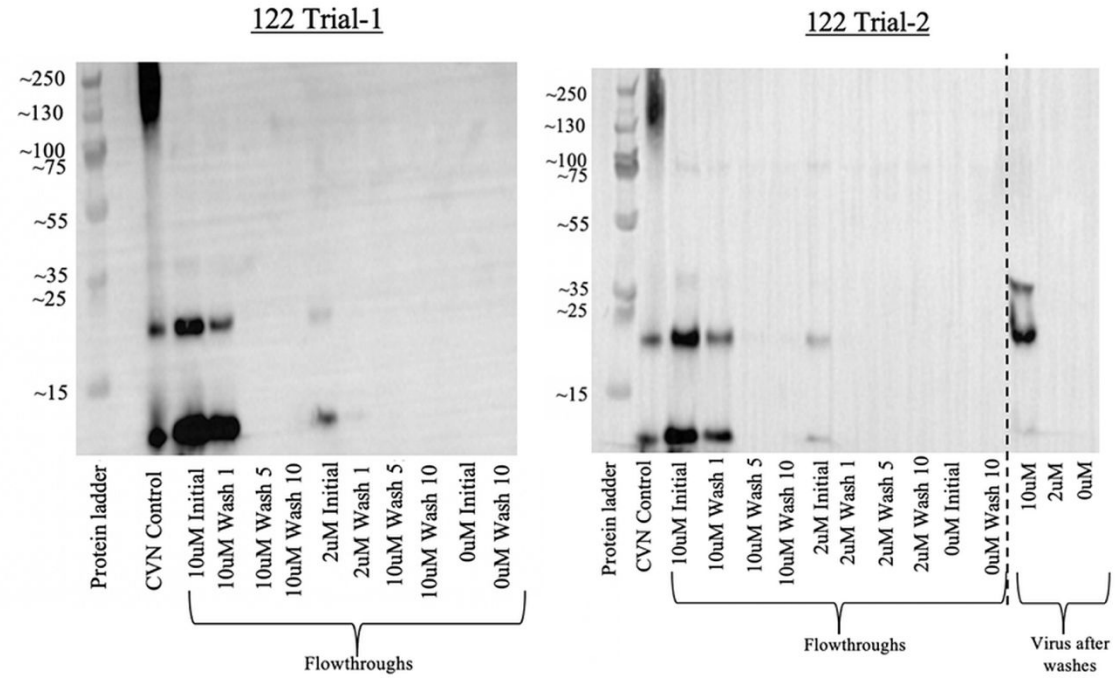

Figure S9: N122D - Western Blot for CV-N detection for Washout Experiments. *Details are given in the legend of Figure S8.*

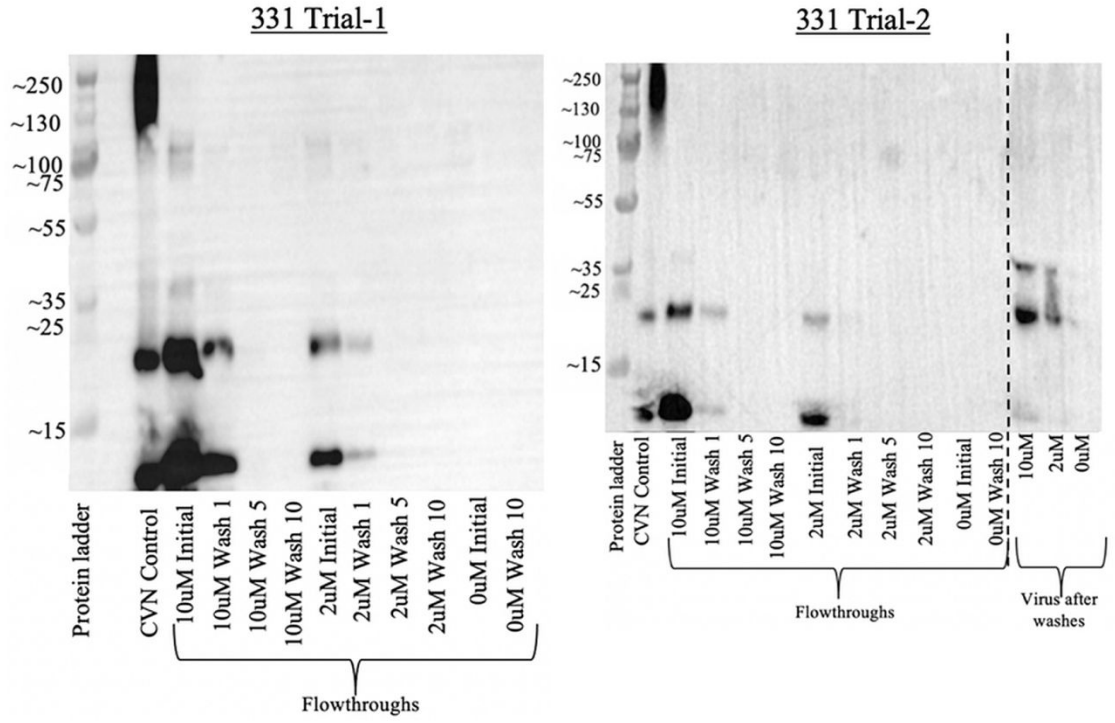

Figure S10: N331D - Western Blot for CV-N detection for Washout Experiments. *Details are given in the legend of Figure S8.*

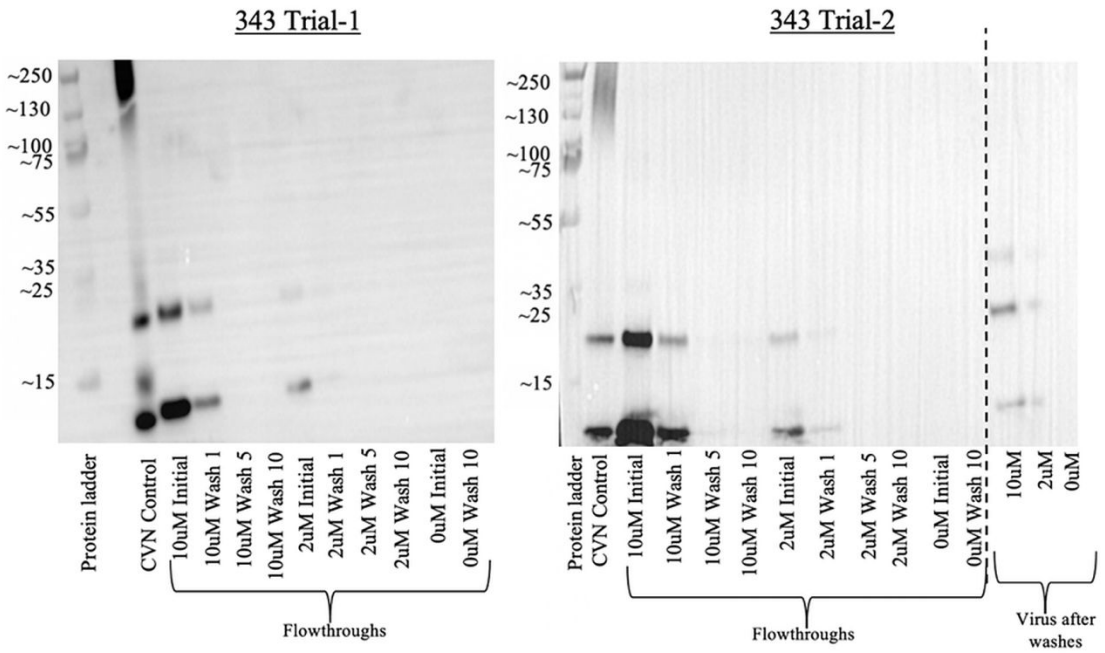

Figure S11: N343D - Western Blot for CV-N detection for Washout Experiments. *Details are given in the legend of Figure S8.*

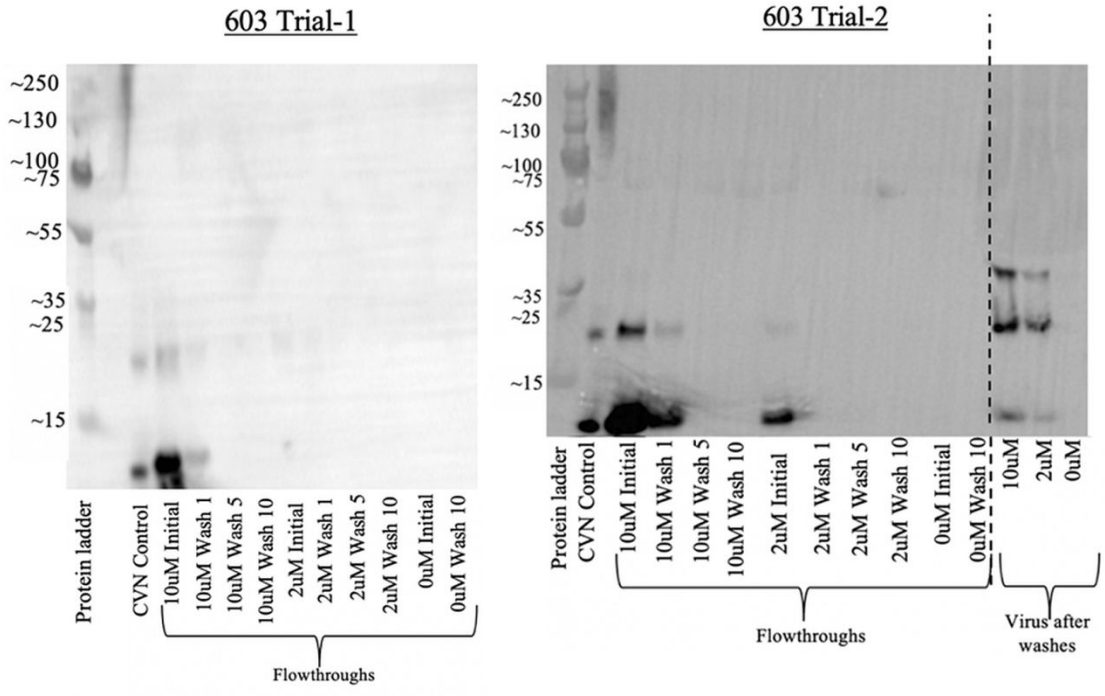

Figure S12: N603D - Western Blot for CV-N detection for Washout Experiments. *Details are given in the legend of Figure S8.*

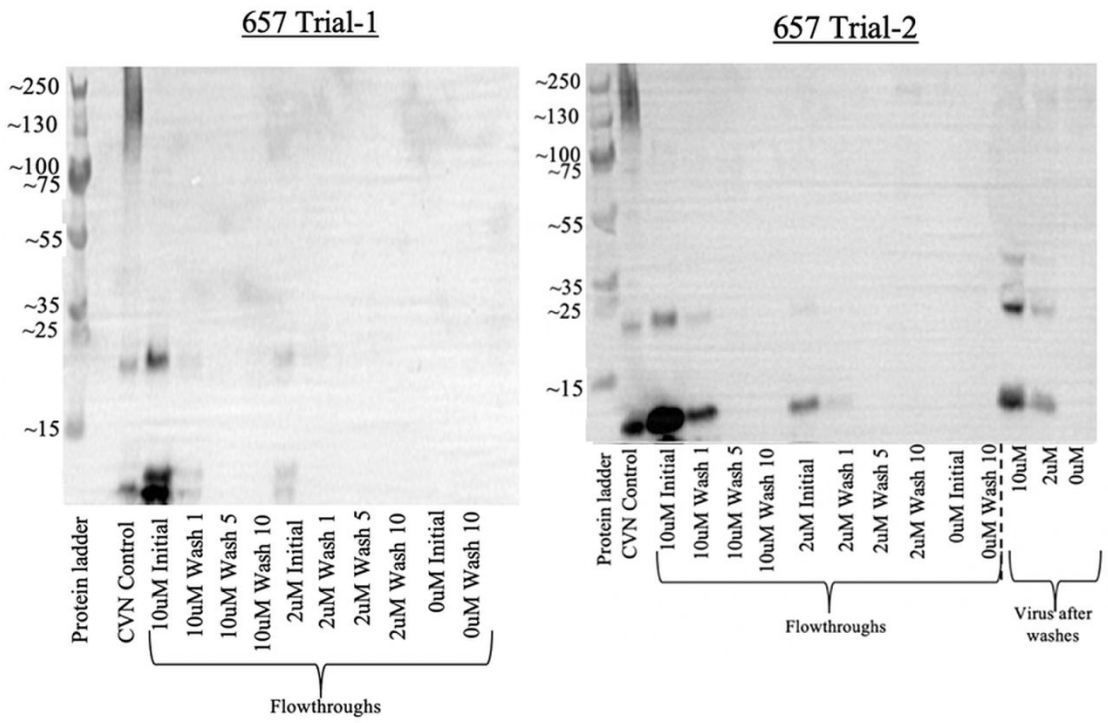

Figure S13: N657D - Western Blot for CV-N detection for Washout Experiments. *Details are given in the legend of Figure S8.*